

Electronic Supplementary Information

Rational Design of Multivalent Biosensor Surfaces to Enhance Viral Particles

Capture

Wenwei Pan^{a,b,c}, Ziyu Han^{a,b}, Ye Chang^{a,b}, Xu Yan^{a,b}, Feng Zhou^{a,b}, Sihong Shen^{a,b}, Xuexin

Duan^{a,b,c,*}

a. State Key Laboratory of Precision Measuring Technology and Instruments, Tianjin University, Tianjin 300072, China.

b. College of Precision Instrument and Opto-electronics Engineering, Tianjin University, Tianjin 300072, China.

c. Department of chemistry, school of science, Tianjin University, Tianjin 300072, China.

* Corresponding author

Tel. /Fax: +86-22-27401002.

E-mail address: xduan@tju.edu.cn

1. Characterizations of 2D-PET

The synthesis schemes of 2D-PET are the same as in our previous work.^{1,2} The chemical structure of 2D-PET and 3D-PETx were verified by ¹H NMR in D₂O (Figure S1). δ [ppm] = 1.32-1.45 (lysine γ -CH₂), (biotin, β -CH₂-), 1.47-1.88 (lysine β , δ -CH₂), (biotin, γ -CH₂), 2.16 (biotin, -CH₂ C(O)NH-), 2.55 (coupled PEG, -CH₂ -C(O)-N), 2.71 (lysine,(-CH₂-C(O)-N)), 2.79-2.88 (lysine, -CH₂-NH-C(O)), (PEG,-CH₂-NH-C(O)), 3.07 (biotin, -S-CH₂-), 3.22 (biotin, -S-CH-), 3.25 (free lysine, -N-CH₂), 3.55 (PEG, CH₂ -O-), 4.12 (lysine, N-CH-C(O)-), 4.29 and 4.47 (biotin, 2 bridge head CH)).

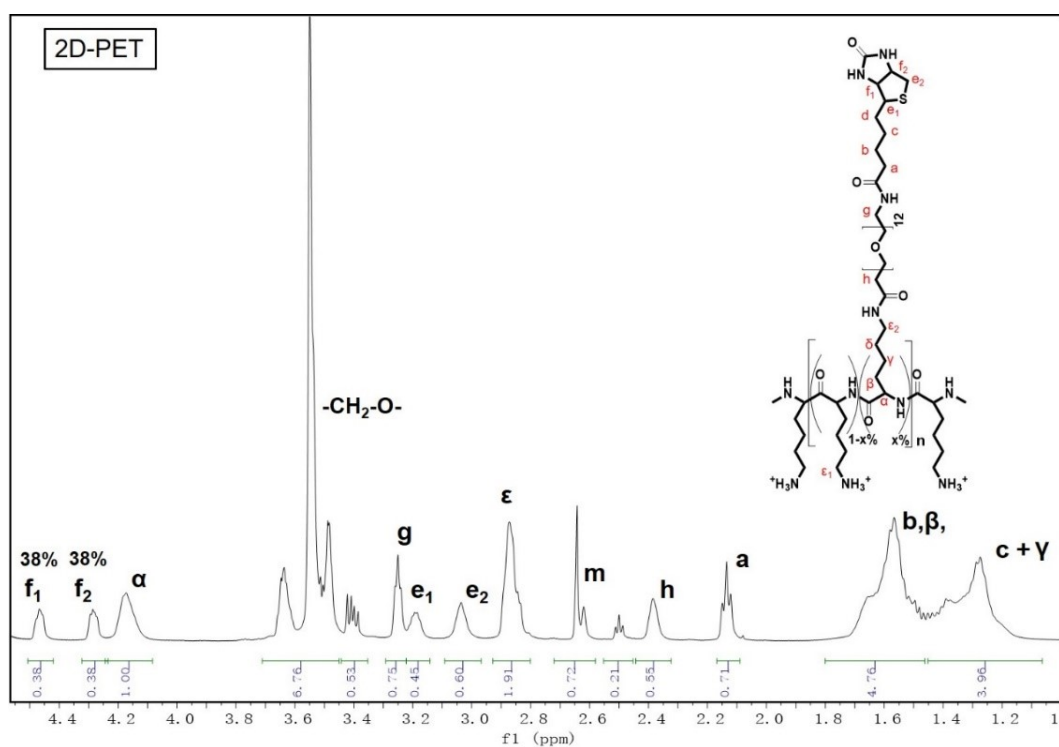


Figure S1. The NMR results of 2D-PET.

2. Characterizations of 3D-PETx

The synthesis schemes of 3D-PETx are the same as in our previous work.² The chemical structure of 3D-PETx were verified by ¹H NMR in D₂O (Figure S2). δ [ppm] = 1.33-1.43 (lysine γ -CH₂), (biotin, β -CH₂-), 1.46-1.91 (lysine β , δ -CH₂), (biotin, γ -CH₂), 2.14 (biotin, -CH₂ C(O)NH-), 2.53 (coupled PEG, -CH₂ -C(O)-N), 2.70 (lysine,(-CH₂-C(O)-N)), 2.82–2.90 (lysine, -CH₂-NH-C(O)), (PEG,-CH₂-NH-C(O)), 3.11 (biotin, -S-CH₂-), 3.21 (biotin, -S-CH-), 3.23(free lysine, -N-CH₂), 3.37 (PEG,-O-CH₃), 3.57 (PEG, CH₂ -O-), 4.14 (lysine, N-CH-C(O)-), 4.24 and 4.47 (biotin, 2 bridge head CH)), 7.88 (triazole H, C=CH-N-).

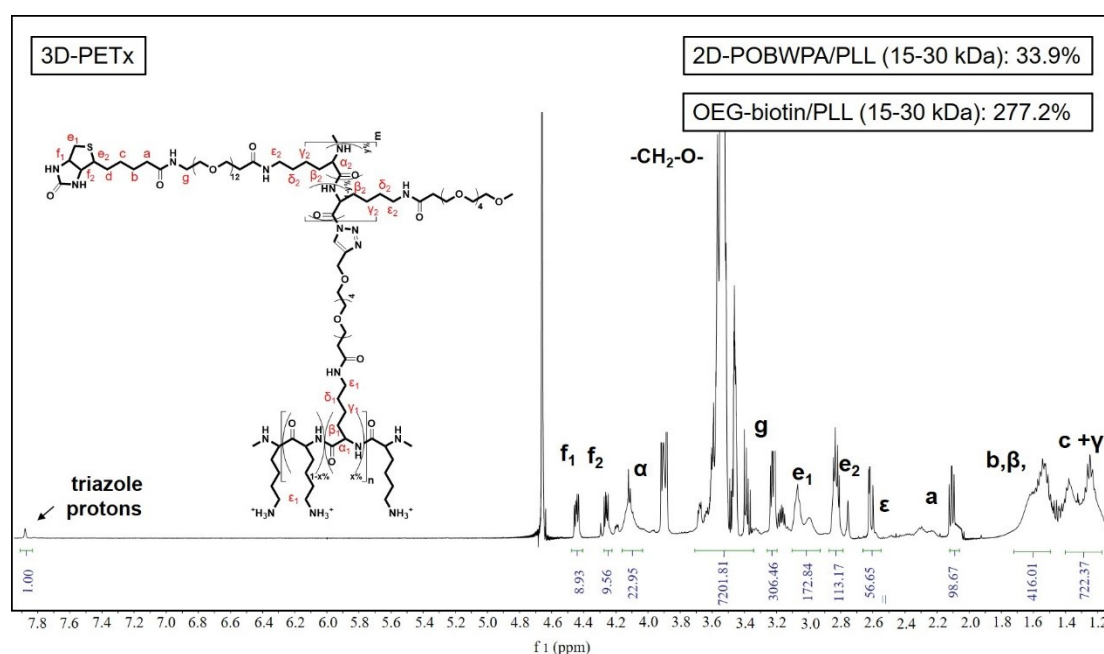


Figure S2. The NMR results of 3D-PETx.

3. Characterizations of 3D-PETy

The chemical structure of 3D-PETy was verified by ^1H NMR in D_2O (Figure S3). δ [ppm] = 1.34-1.42 (lysine γ - CH_2), (biotin, β - CH_2 -), 1.44-1.89 (lysine β , δ - CH_2), (biotin, γ - CH_2), 2.12 (biotin, - CH_2 C(O)NH-), 2.53 (coupled PEG, - CH_2 -C(O)-N), 2.72 (lysine,(- CH_2 -C(O)-N)), 2.83-2.91 (lysine, - CH_2 -NH-C(O)), (PEG,- CH_2 -NH-C(O)), 3.10 (biotin, -S- CH_2 -), 3.22 (biotin, -S-CH-), 3.23(free lysine, -N- CH_2), 3.38 (PEG,-O-CH₃), 3.59 (PEG, CH_2 -O-), 4.15 (lysine, N-CH-C(O)-), 4.27 and 4.48 (biotin, 2 bridge head CH)) , 7.88 (triazole H, C=CH-N-).

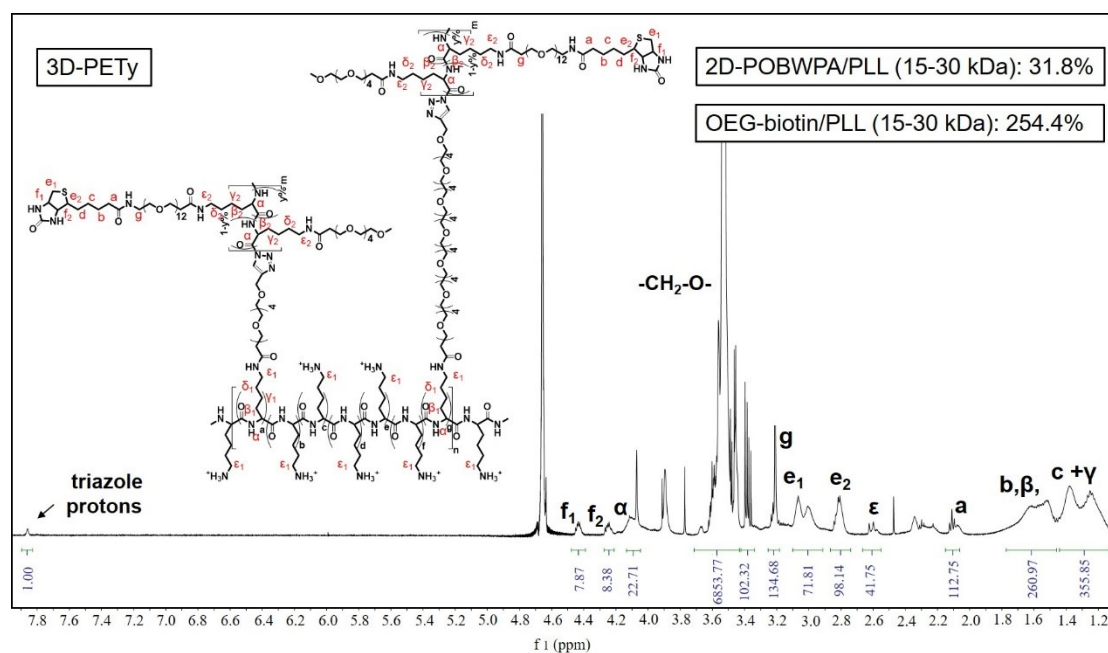


Figure S3. The NMR results of 3D-PETy.

4. Non-specific Bindings on Biosensing Surfaces

In order to clarify the contribution of non-specific interactions to Blitz measurements, antibodies not labeled with biotin were used as nonspecific proteins, and their binding to polyelectrolyte-based biosensing surfaces were studied. In the experiment, the Blitz fibers were sequentially immersed in polyelectrolyte (1mg/mL), SAV (200 nM), and antibody solution (200 ug/mL). After each step, there was a buffer cleaning step. Figure S4 shows the real-time Blitz measurement of antibody binding. The results showed that nonspecific antibodies hardly bind to the biosensor surface. This is not only due to the rich antifouling group (polyethylene glycol) on the biosensor surface, but also due to the excessive amount of SAV covering all exposed sensing areas. Therefore, in this work, the effect of non-specific interactions in Blitz experiments can be ignored.

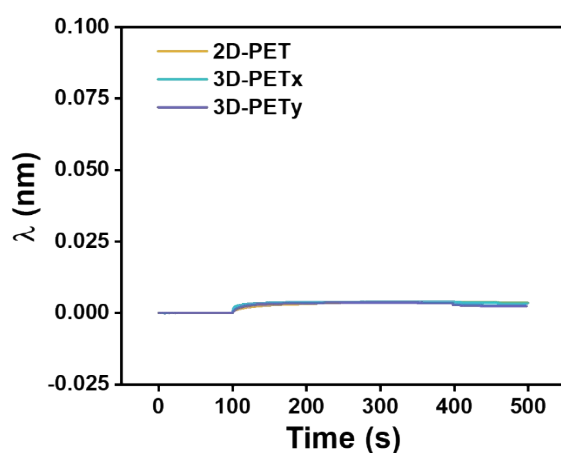


Figure S4. Real time Blitz measurement of non-specific bindings on different polyelectrolyte-based biosensing surfaces

5. AFM Measurements of Coronavirus on 2D-PET and 3D-PETy Based Biosensing Interfaces.

Figure S5a and S5b are the AFM height images of 2D-PET and 3D-PETx coatings without viral sample treatment, respectively. The results showed that the morphology of 3D-PETx and 3D-PETy surfaces without virus sample treatment were uniform, and their mean roughness (R_a) in the scan area ($5\ \mu\text{m}^2$) is 0.517 nm and 0.625 nm, respectively. Furthermore, the stiffness of the coronavirus immobilized on polyelectrolyte-initialized flat silicon (Si/SiO_2) substrates were measured (Figure S5c and S5d). The measured stiffness results show that pie-like objects were much softer relative to the surrounding plane, suggesting they are viral particles. And, the morphology of the virus on the substrate was consistent with the AFM height measurements.

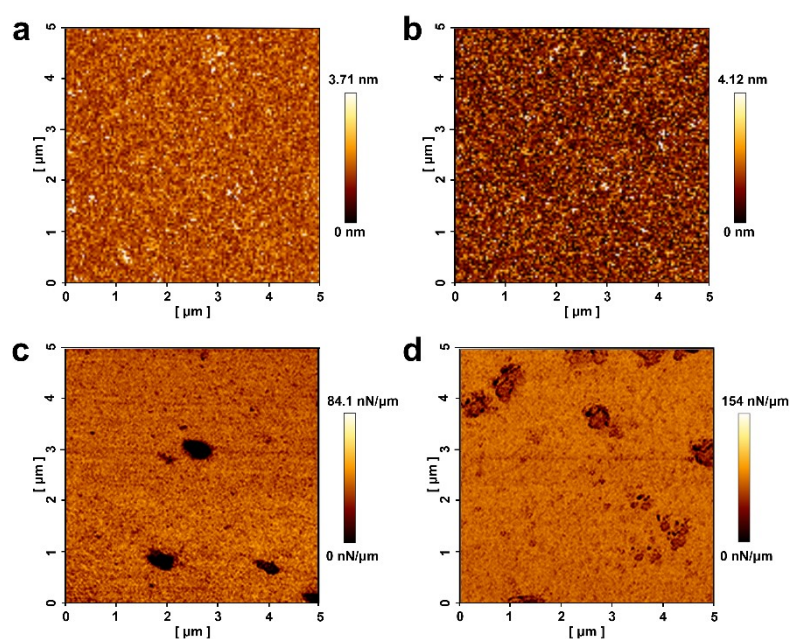


Figure S5. (a, b) AFM height images of 2D-PET and 3D-PETx coatings without viral sample treatment, respectively; (c) AFM stiffness maps of virus on 2D-PET coating; (d) AFM stiffness maps of virus on 3D-PETx coating.

6. AFM Height Measurements of Covalently Immobilized Coronavirus on Substrates.

The coronaviruses were covalently immobilized on the flat gold-plated silicon substrates by thiol-Au chemistry. And, the results of AFM height measurement showed that the virus was successfully immobilized on the substrate (Figure S6).

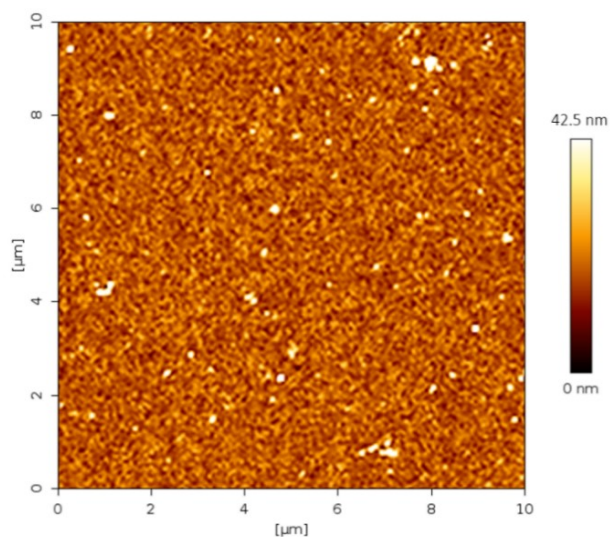


Figure S6. Height map of the virus immobilized on the surface of the substrates.

7. Dynamic Binding Force Measurement on the 3D Biosensing Interfaces.

In the experiments, the SP-antibody functionalized AFM probes were approached and retracted from the sample to quantify the dynamic binding force in HEPES buffer at 37 °C. And, we measure the dynamic binding force of 4225 points on an area of 100 μm^2 .

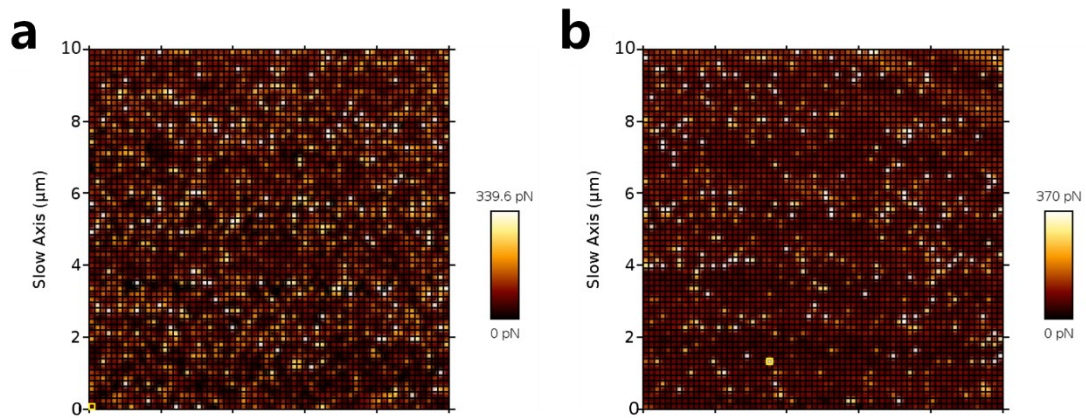


Figure S7. Dynamic binding force measurement on 3D-PETx b) and 3D-PETy c) based surface.

8. Robustness of 3D-PETy Coatings on Sensor Surfaces

SAv binding experiments were used to investigate the robustness of 3D-PETy coatings. In the experiment, twelve 3D-PETy-immobilized Blitz fibers were divided into four equal groups and immersed in HEPES buffer to undergo rinsing steps for up to 2, 8, 16 and 24 hours, respectively. Figure S8a shows the real-time binding of fibers to SAv after the rinsing steps. Figure S8b reflects the effect of rinsing steps of different durations on SAv binding. The results showed that the 3D-PETy coating was firmly immobilized on the sensor surface even after immersion rinsing for up to 24 hours, achieving stable binding to SAv.

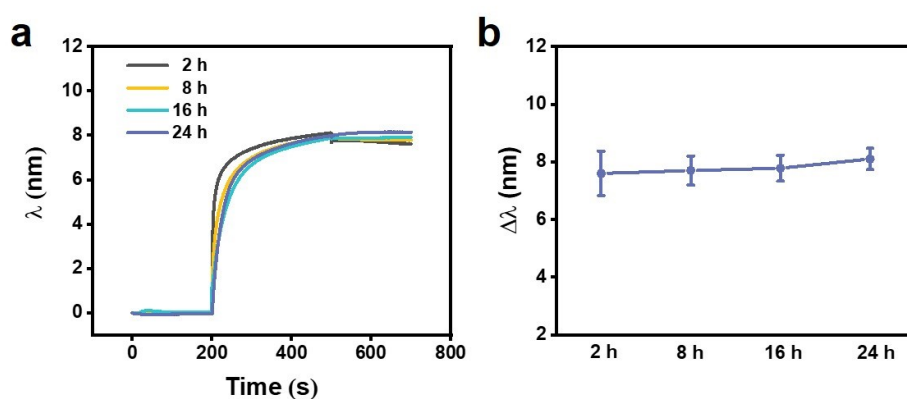


Figure S8. (a) The real-time binding of probes to SAv after rinsing steps of different durations and (b) the effect of rinsing steps of different durations on SAv binding. Error bars represent standard deviation, $n=3$.

9. References

- (1) Z. Han, Y. Wang and X. Duan, *Anal. Chim. Acta.*, 2017, 964, 170-177.
- (2) W. Pan, Z. Han, Y. Chang and X. Duan, *Biosens. Bioelectron.*, 2020, 167, 112504.